HHS Public Access

Author manuscript

Exp Neurol. Author manuscript; available in PMC 2024 July 02.

Published in final edited form as:

Exp Neurol. 2022 November ; 357: 114173. doi:10.1016/j.expneurol.2022.114173.

Aging astrocytes metabolically support aging axon function by proficiently regulating astrocyte-neuron lactate shuttle

Chinthasagar Bastian[b], **Sarah Zerimech**[a], **Hung Nguyen**[a], **Christine Doherty**[b], **Caroline Franke**[b], **Anna Faris**[b], **John Quinn**[b], **Selva Baltan**[a,b,*]

[a]Anesthesia and Perioperative Medicine, Oregon Health and Science University, Portland, OR 97239, United States of America

[b]Department of Neurosciences, Cleveland Clinic Foundation, Cleveland, OH 441952, United States of America

Abstract

The astrocyte-neuron lactate shuttle (ANLS) is an essential metabolic support system that uptakes glucose, stores it as glycogen in astrocytes, and provides glycogen-derived lactate for axonal function. Aging intrinsically increases the vulnerability of white matter (WM) to injury. Therefore, we investigated the regulation of this shuttle to understand vascular-glial metabolic coupling to support axonal function during aging in two different WM tracts. Aging astrocytes displayed larger cell bodies and thicker horizontal processes in contrast to thinner vertically oriented processes of young astrocytes. Aging axons recovered less following aglycemia in mouse optic nerves (MONs) compared to young axons, although providing lactate during aglycemia equally supported young and aging axonal function. Incubating MONs in high glucose to upregulate glycogen stores in astrocytes delayed loss of function during aglycemia and improved recovery in both young and aging axons. Providing lactate during recovery from aglycemia unmasked a metabolic switch from glucose to lactate in aging axons. Young and aging corpus callosum consisting of a mixture of myelinated and unmyelinated axons sustained their function fully when lactate was available during aglycemia and surprisingly showed a greater resilience to aglycemia compared to fully myelinated axons of optic nerve. We conclude that lactate is a universal substrate for axons independent of their myelination content and age.

[*]Corresponding author at: Anesthesia and Perioperative Medicine (APOM), Mackenzie Hall 2140A, Oregon Health & Science University, Mail Code: L459, 3181 S. W. Sam Jackson Park Rd., Portland, OR 97239, United States of America. baltan@ohsu.edu (S. Baltan).

CRediT authorship contribution statement

Chinthasagar Bastian: Writing – review & editing. **Sarah Zerimech:** Data curation, Formal analysis. **Hung Nguyen:** Data curation, Formal analysis. **Christine Doherty:** Data curation, Formal analysis. **Caroline Franke:** Visualization, Investigation. **Anna Faris:** Data curation, Formal analysis. **John Quinn:** Data curation, Formal analysis. **Selva Baltan:** Conceptualization, Visualization, Investigation, Formal analysis, Writing – review & editing.

Declaration of Competing Interest

The authors declare that there is no conflict of interest.

Appendix A. Supplementary data

Supplementary data to this article can be found online at https://doi.org/10.1016/j.expneurol.2022.114173.

Keywords

Aglycemia; Aging; Astrocyte; Lactate; White matter

1. Introduction

White matter (WM) is specialized in structure and function to coordinate their cellular components and electrically-active axons with their supporting glial cells to respond to metabolic challenges. Interestingly, studies over the past 20 years have unraveled mechanisms exclusive to the central nervous system (CNS) where astrocytic end-feet enwrapping capillaries contribute to the structure and function of the blood-brain barrier (BBB) (Andriezen, 1893; Cajal, 1909; Peters and Palay, 1991) and also specialize in supporting axonal function. Perivascular astrocytic end-feet take up glucose via glucose transporter 1 (GLUT 1) to actively regulate glycogen stores such that high ambient glucose upregulates glycogen and low levels of glucose deplete glycogen stores (Bastian et al., 2019; Brown et al., 2003b; Tekkok et al., 2005). A rapid breakdown of glycogen into lactate during increased neuronal activity or under low glucose conditions becomes essential for maintaining axonal function (Dringen and Hamprecht, 1993; Magistretti et al., 1993). This process was first proposed by Pellerin and Magistretti in 1994 (Magistretti et al., 1994) and was named the Astrocyte-Neuron Lactate Shuttle (ANLS) to accurately describe metabolic support between astrocytes and neurons (Fig. 1).

Lactate is an energetically-favorable substrate for neurons because of their high cellular activity, as it is able to circumvent the energetic costs involved in the early steps of glycolysis, entering the tricarboxylic acid cycle after its conversion to pyruvate (Bolanos et al., 2010). Therefore, neurons can even opt to import lactate over glucose when both are available (Bouzier-Sore et al., 2006), perhaps pertaining to the role of lactate in maintaining synaptic activity in neurons (Schurr et al., 1988). Further studies supporting the unidirectional transport of lactate confirmed cell-specific monocarboxylate transporter (MCT) expression, generally MCT1 in astrocytes to extrude lactate to the extracellular space and MCT2 on axons to pick up lactate (Broer et al., 1997; Poole et al., 1996) (Deitmer et al., 2019; Ferguson et al., 2018). Astrocytes are the storehouses for glycogen in the CNS (Cataldo and Broadwell, 1986; Magistretti et al., 1993; Peters and Palay, 1991); when compared to neurons, astrocytes exhibit a higher rate of glycolysis and thus can synthesize more lactate (Amaral et al., 2011; Walz and Mukerji, 1988). In addition, enzymes of glycolysis (Halim et al., 2010; Herrero-Mendez et al., 2009; Itoh et al., 2003), glycogen metabolism (Pellegri et al., 1996; Pfeiffer-Guglielmi et al., 2003), and low levels of malate-aspartate shuttle activity (Berkich et al., 2007; Ramos and Colquhoun, 2003) provide necessary machinery for lactate production from glycogen in astrocytes. The glycogen content in astrocytes directly correlates to the ability of axons to sustain function, and aglycemia leads to axonal failure due to rapid degradation of glycogen stores (Brown et al., 2003a). Expectedly, providing lactate during aglycemia preserves axonal function (Tekkok et al., 2005). Thus, astrocytic glycogen is dynamically regulated and is crucial for supplying energy to axons under both pathological and physiological conditions.

Axons, together with their mitochondria and associated myelin, undergo prominent structural and functional changes with aging and become more vulnerable to metabolic insults such as ischemia (Baltan, 2014; Stahon et al., 2016). Aging has been shown to cause prominent changes in astrocytes (Fabricius et al., 2013; Lindsey et al., 1979); therefore, it is plausible that aging astrocytes fail to perform their role in the ANLS and that this impaired astrocyte-axon metabolic interaction renders WM vulnerable to energy deprivation. The neurovascular unit (NVU) is an intricate structure composed of neurons, astrocytes, microglia, oligodendrocytes, endothelial cells, pericytes, smooth muscle cells, and brain-specific extracellular matrix (ECM). Astrocytes are strategic members of the NVU, as they pick up vascular glucose either to store as glycogen for conversion to lactate or convert it to lactate instantly to support axonal function when there is increased activity or when glucose is low/absent. Therefore, the ANLS is an important example of astrocyte-axon metabolic coupling while connecting the NVU to brain metabolism and function. Oligodendrocytes are another critical member which also utilizes both glucose and lactate as a source of energy (Sanchez-Abarca et al., 2001). Furthermore, compelling evidence shows that oligodendrocytes also deliver lactate to axons, establishing an oligodendrocyte-axon lactate metabolic coupling to show how white matter components cooperate to sustain NVU (Saab et al., 2016). Impairment of the oligodendrocyte-axon lactate shuttle is proposed to contribute to chronic demyelinating and psychiatric diseases (Nave and Ehrenreich, 2014). Endothelial cells as part of the BBB express MCT1 in luminal and abluminal surfaces (Bergersen, 2015; Pellerin et al., 1998). Under physiological conditions, astrocytes produce and release lactate in the extracellular matrix but in order to maintain low extracellular levels, excess lactate is transferred into the blood circulation through MCT-1 expressed at the surface of endothelial cells (Adijanto and Philp, 2012). The impact of aging on MCT1 expression, endothelial regulation of lactate, and oligodendrocyte-axon lactate shuttle efficiency are yet to be explored. To assess whether aging astrocytes sustain their role of providing lactate to neurons and whether glycogen-derived lactate differentially supports axons based on age and myelin content, we compared the axonal electrical response to aglycemia in mouse optic nerves (MONs), a pure myelinated WM tract, and corpus callosum (CC) slices. We show that aging axons become more vulnerable to the absence of glucose, although they can use lactate as an alternative fuel more efficiently than young axons. Aging astrocytes efficiently perform their role to regulate their glycogen stores and to provide lactate to support aging axonal function during aglycemia. Providing lactate during recovery from aglycemia reveals a metabolic switch from glucose to lactate in aging axons. Interestingly, CC axons show greater resilience to aglycemia and readily switch to lactate as an alternate substrate when glucose is not available. We conclude that the increased vulnerability of aging optic nerve axons to aglycemia is mainly due to a metabolic switch in axon energy metabolism, rather than the failure of aging astrocytes to support the ANLS. Lactate emerges as a universal alternative substrate buffer for young and aging axons independent of their myelination content.

2. Materials and methods

2.1. Animals and chemicals

All experimental procedures were performed according to the principles of the Guide for the Care and Use of Laboratory Animals (National Association for Biomedical Research) and approved by The Institutional Animal Care and Use Committee (IACUC) of the Cleveland Clinic. Experimental procedures were performed and reported in compliance with the ARRIVE guidelines (Animal Research: Reporting In Vivo Experiments). All chemicals used for electrophysiology experiments were purchased from Millipore-Sigma (St. Louis, MO). C57BL/6 J adult male mice (2–3 months old, “young”; and 12 months old, “aging”) were purchased from Jackson Laboratory (USA) and housed in the Cleveland Clinic animal facility under a 12 h-light/dark cycle with food and water available ad libitum.

2.2. Electrophysiology and glucose deprivation

Electrophysiology experiments in mouse optic nerves (MON) (Baltan, 2014; Baltan et al., 2018; Baltan et al., 2008; Baltan et al., 2013; Baltan et al., 2011b; Bastian et al., 2018a; Bastian et al., 2018b; Bastian et al., 2018c; Stahon et al., 2016) and corpus callosum slices (Baltan, 2006; Tekkok and Goldberg, 2001; Tekkok and Ransom, 2004) were performed as previously described (Tekkok and Goldberg, 2001). Briefly, animals were randomly picked and MONs were obtained from adult male C57BL/6 J mice at 2–3 months or 12 months of age. Following CO_2 asphyxiation of mice, MONs were freed from their dural sheaths, placed in a Haas top perfusion chamber (Harvard Apparatus, Holliston, MA), and superfused with artificial cerebrospinal fluid (ACSF) with the following composition (in mM): 124 NaCl, 3 KCl, 2 $CaCl_2$, 2 $MgCl_2$, 1.25 NaH_2PO_4, 23 $NaHCO_3$, and 10 D-glucose, at 37 °C. MONs were allowed to equilibrate for at least 15 min in the recording chamber in normal ACSF before further experimentation, all performed at 37 °C. Glass suction electrodes filled with ACSF were used for stimulating (Isostim520; WPI, Sarasota, FL) and for recording compound action potentials (CAPs). The recording electrode was connected to an Axoclamp 900A amplifier (Molecular Devices, LLC, Sunnyvale, CA) and signals were amplified 20 or 50 times, filtered at 3 kHz, and acquired at 20–30 kHz (SR560, Stanford Research Systems, Sunnyvale, CA). Stimulus pulse strength (30 μs duration) was adjusted to evoke the maximum CAP possible and then increased another 25% for supra-maximal stimulation. During experiments, the supramaximal CAP was elicited every 30s.

For corpus callosum (CC) slice electrophysiology experiments, male C57BL/6 J mice at 2–3 months (young) or 12 month of age (aging), were decapitated following deep CO_2 anesthesia, following which the brains were dissected out immediately into ice-cold ACSF oxygenated with a mixture of 95% O_2/5% CO_2. The whole brain was placed on the platform of the vibratome (Leica VT1000S, Buffalo Grove, IL) and 400-μm-thick coronal slices were cut. Only the slices (8–10/brain) in which the anatomical structure of the corpus callosum was visualized clearly were included in the experiments. Slices were allowed to stabilize for at least 2 h at room temperature (22–23 °C) before they were transferred to a Haas-type slice chamber (Harvard Apparatus, Holliston, MA) kept at 33–34 °C. CAPs across the corpus callosum were evoked by using a bipolar tungsten stimulation electrode (Microprobes,

Gaithersburg, MD) and were recorded by an extracellular electrode filled with 2 M NaCl (Baltan, 2006; Tekkok and Goldberg, 2001; Tekkok and Ransom, 2004).

Aglycemia was induced by switching to a glucose-free ACSF (replaced with equimolar sucrose to maintain osmolarity). Following 60 min of aglycemia, ACSF was restored and CAPs were recorded for up to 5 h. Clampfit version 10.2 (Molecular Devices, LLC, Sunnyvale, CA) was used to measure the area under the CAP, which best represents the measure of the number of active axons (Baltan, 2014; Baltan et al., 2018; Baltan et al., 2008; Baltan et al., 2013; Baltan et al., 2011b; Bastian et al., 2018a; Bastian et al., 2018b; Bastian et al., 2018c; Stahon et al., 2016). Investigators were blinded to the groups. For comparing the CAP area between control and experimental groups, an average of 10 CAPs at baseline was measured. CAP areas from each experiment were normalized to baseline control levels for studying recovery after aglycemia. Experiments in the same group were pooled together, and the percentage of recovery was calculated in the normalized group's time course. The recovery was monitored throughout and the recovery time point at the end of experiments was used for comparison between groups.

2.3. Immunohistochemistry

Immunohistochemistry (IHC) experiments were conducted by standard methods used routinely in our laboratory (Baltan, 2012; Baltan et al., 2011a; Baltan et al., 2011b; Bastian et al., 2018b; Bastian et al., 2018c; Murphy et al., 2014) with MONs collected after 5 h following aglycemia. Briefly, MONs were perfusion-fixed (4% paraformaldehyde and 0.025% glutaraldehyde) and cryosectioned. Sections of 16 μm thickness were blocked in 5% normal goat/donkey (50% by volume) serum (Millipore Sigma, St-Louis, MO) and 0.3% Triton X-100 (Millipore Sigma, St-Louis, MO) for 60 min at room temperature. Sections were then incubated in primary antibody against the glial fibrillary acidic protein (GFAP) overnight at 4 °C (rabbit, Immunostat Cat No. 22522; 1:15 dilution). Secondary antibodies used were donkey anti-rabbit Cy5 and anti-rabbit Cy3 (Jackson ImmunoResearch Laboratories, Inc., West Grove, PA) prepared in 2% normal goat serum for 2 h. Nuclei of these permeabilized cells were counterstained using Sytox Green Stain (EMD Millipore, Cat. No. 57020; 1:25000 dilution).

2.4. Imaging and analysis

A Leica DMI6000 inverted confocal laser-scanning microscope (Buffalo Grove, IL) was used for digital image acquisition. Argon and He–Ne lasers were used to excite Sytox Green (488 nm line), Cy3 (543 nm line), and Cy5 (647 nm line). Two to three adjacent sections from each MON were imaged for a total of five areas of interest (AOI). A total of 10–16 optical sections, each of 1 μm thickness at 1024 pixel by 1024 pixel size, were collected in the z-axis using a 40× (HCX APO, water immersion; numerical aperture, 0.80; Leica, Buffalo Grove, IL) objective lens under set gain, laser power, pinhole, and photomultiplier tube (PMT) settings for all groups.

2.5. Lactate concentration detection

Lactate-Glo™ Assay (Promega #J5021 Madison, WI) was used to detect lactate concentration according to the manufacture protocols. At the end of electrophysiology

experiments, MONs were flash-frozen with liquid nitrogen and stored at −80 °C until the day of experiment. A pair of MONs were homogenized (749540–0000 Pellet pestle motor, DWK Life Sciences, Millville, NJ) on ice in 75 μl of homogenization buffer (Promega #J5021 Madison, WI). A small aliquot was then centrifuged at 14,000 rpm for 10 min, the supernatant was collected, and the protein concentration was estimated using Qubit Protein Assays (ThermoFisher, Waltham, MA). Homogenized samples were diluted to approximately 25 μg protein in 50 μL of dilution buffer (Promega #J5021 Madison, WI). Samples were incubated with 50 μL of Lactate Detection Reagents for 60 min at room temperature protected from light. The lactate concentration was detected using luminescence reader (Spectramax iD3, Molecular Devices, San Jose, CA). All samples are done in triplicate.

2.6. Statistical analysis

All summarized data are presented as mean ± SD. Graphpad Prism version 5.0f (Graphpad Software, Inc., La Jolla, CA) was used for statistical analysis. The number of MONs or CC slices (n numbers) required for the study was estimated using power analysis (set at 80% and $\alpha = 0.05$). Data conform to normality as per the two-tailed Student's *t*-tests (Figs. 2D, 3B, D, 4B, C, E, F, 5B, D, 6E, G, H, 7E, H, G and 8B) or one-way ANOVAs with a Newman-Keuls *post-hoc* test (Fig. 4G and 5E) as appropriate. Differences were considered to be significant at $p < 0.05$. The *p*-values and significance values are indicated individually for each figure in the text.

3. Results

3.1. Aging WM is more vulnerable to aglycemia

The isolated optic nerve, which is a purely myelinated WM tract (Foster et al., 1982), has been an ideal ex vivo preparation to quantify axonal function using electrophysiology and to study WM cellular structure and cytoskeleton using immunohistochemistry and fluorescence imaging (Baltan, 2012; Baltan et al., 2011a; Baltan et al., 2008; Baltan et al., 2011b; Bastian et al., 2018b; Bastian et al., 2018c; Murphy et al., 2014; Tekkok et al., 2007). Moreover, the optic nerve is sensitive to the aging process (Cavallotti et al., 2003; Cavallotti et al., 2002), so it is useful for studying the effects of age on WM structure and function (Baltan, 2012; Baltan et al., 2008; Bastian et al., 2018b; Bastian et al., 2018c; Stahon et al., 2016). We evaluated the effects of aging on astrocytes in MONs obtained from 2-month-old and 12-month-old mice using immunohistochemistry and anti-GFAP antibody with confocal imaging. GFAP (+) astrocytes position themselves in a specific manner among myelinated axons. GFAP occupies about 15% of astrocytic volume and is present in large/proximal processes, while distal and fine peripheral processes are devoid of GFAP However, GFAP detection via immunohistochemistry is more prominent in white versus gray matter astrocytes and does label all astrocytic processes (Bushong et al., 2004). We urge the reader to keep in mind at all times that now on we refer to GFAP-stained processes as processes for simplicity. In young MONs, GFAP (+) astrocytes were small in size with thin processes extending vertically to parallel running axons (Fig. 2A, Young, green for GFAP (+) astrocytes). On the other hand, aging astrocytes that increase in body size had thicker and longer processes that ran parallel to the axons (Fig. 2A, Aging, compare

merged and zoomed images, yellow arrowheads indicate axonal run). The Sytox (+) nuclei (as pre permeabilization for IHC, all the nuclei) showed no change in size, but a decrease in number as previously reported (Baltan, 2014). To determine the extent to which these structural changes of aging astrocytes affect their performance in sustaining the ANLS, the effects of aglycemia on axonal function recovery were determined in MONs from 2-month-old and 12-month-old mice. The functional integrity of MON axons was monitored by quantifying the area under CAPs evoked by a supramaximal stimulus. Note that aging axons displayed larger CAPs with prominent increases in amplitude and duration (Fig. 2B, Aging, red, baseline) compared to young axons (Fig. 2B, Young, green, baseline) as previously reported (Stahon et al., 2016). After a 30-min baseline recording, aglycemia was introduced by superfusing MONs in ACSF in which glucose (10 mM) was replaced with equimolar sucrose. The MONs were then superfused with glucose-containing ACSF for 5 h. The CAP area remained unchanged for ~30 min after the onset of aglycemia and then gradually diminished and completely disappeared in ~55 min. Note that it is the glycogen-derived lactate delivery by astrocytes that sustains axon function (Tekkok et al., 2005) and therefore glycogen levels regulate the duration of axon function during aglycemia (Brown et al., 2003b; Tekkok et al., 2005). We further validated that loss of axon function coincided with complete loss of available lactate levels (Supplemental Fig. 1C). After aglycemia, the CAP area recovered to 36.7 ± 13.3% ($n = 15$) in young MONs (Fig. 2B, green traces (dashed line indicates baseline), 2C green time course, and 2D green dot plot). To evaluate whether aging axons become more vulnerable to reduced glucose availability, aging MONs (12 months old) were exposed to aglycemia (60 min) in a similar manner (Fig. 2B and C). CAP area in aging axons followed an identical time course of functional loss as young axon function during aglycemia, such that axon function was sustained for ~30 min before completely disappearing. However, the CAP area showed minimal recovery (13.3 ± 7%, $n = 10$, $p < 0.001$, Unpaired Student's *t*-test) in aging MONs following aglycemia (60 min; Fig. 2B, red traces, 2C red time course, and 2D red dot plot). Quatification of lactate showed a similar drop in lactate content in young and aging These results suggest that in addition to morphological changes in astrocytes with aging, axons recover less after aglycemia in aging white matter.

3.2. Aging axons efficiently substitute lactate for glucose to sustain function

The efficiency of lactate as an alternate substrate during aglycemia has been confirmed in a series of electrophysiological experiments using MONs obtained from Swiss Webster mice (Brown et al., 2003a; Tekkok et al., 2005). We evaluated the CAP area during aglycemia in C57BL/6 J young mice as a basis for our experiments to compare it with aging mice. Replacing glucose in ACSF with 20 mM lactate (carbon equivalent of 10 mM glucose) fully sustained the CAP area in young (Fig. 3A, blue traces and time course; 3B, blue dot plot, 96.8 ± 15.4%, $n = 4$) and aging (Fig. 3C, brown traces, and time course; 3D, brown dot plot, 93.8 ± 5.6%, $n = 4$) MONs during aglycemia. The ability of lactate to support axon function during aglycemia was in marked contrast to the aglycemia-only condition, where both young (Fig. 3A, green time course and 3B, green dot plot, $p < 0.001$, Unpaired Student's *t*-test) and aging (Fig. 3C red time course, 3D, red dot plot, $p < 0.001$, Unpaired Student's t-test) axons completely ceased to function. These results suggest that aging axons maintain their function using lactate or glucose with equal efficiency and also presume that

MCT1 is expressed and remains functional on aging axons. Note that lactate is provided externally in these experiments, raising the question as to whether aging astrocytes perform their function to convert glycogen to lactate to metabolically sustain aging axons when glucose is unavailable.

3.3. Aging astrocytes effectively shuttle lactate to axons during aglycemia

Astrocyte diligently couple axonal function to the NVU by taking up glucose, storing it as glycogen, and converting it to lactate when glucose is low/absent or when axon function is increased (Brown et al., 2003a; Dringen and Hamprecht, 1993; Magistretti et al., 1993). Furthermore, astrocytes can regulate their glycogen stores such that high ambient glucose levels upregulate glycogen stores, while low glucose levels downregulate or deplete glycogen stores (Brown et al., 2003a; Tekkok et al., 2005). We verified this metabolic coupling role of astrocytes in young C57BL/6 J mice by incubating optic nerves in high glucose ACSF (30 mM glucose) for 30 min to upregulate their glycogen levels (Fig. 4A, young, pink traces and time course). After the onset of aglycemia, CAP area showed a prominent delay to plummet during aglycemia after incubating young MONs in 30 mM glucose (Fig. 4A, Young, pink time course, 4C, pink dot plot, 35.1 ± 5.4 min, $n = 4$) compared to MONs kept in 10 mM glucose (Fig. 4A, green time course, 4C, green dot plot, 22 ± 6.1, $n = 14$, $p < 0.01$, Unpaired Student's *t*-test). Moreover, despite the decline in CAP area after the onset of aglycemia, a portion of CAP area was preserved at the end of 60 min (~10%, Fig. 4A, pink trace, "b"). Following aglycemia, CAP area showed a prominent recovery in MONs kept in 30 mM glucose in contrast to MONs kept in 10 mM (Fig. 4B, young, 66.8 ± 6.9%, n = 4, 30 mM glucose versus 36.7 ± 13.3%, n = 14, 10 mM glucose, $p < 0.001$, Unpaired Student's t-test). Strikingly, aging MONs showed an identical resistance to aglycemia after incubation in 30 mM glucose (Fig. 4D, cyan traces and time course). The decline in CAP area in aging MONs followed a similar delay as in young MONs after the onset of aglycemia (Fig. 4D, Aging 30 mM glucose, cyan time course, 4E, cyan dot plot, 38.8 ± 2.1 min, n = 4 versus Aging 10 mM glucose, Fig. 4D red time course, 4C, red dot plot, 23.7 ± 2.3 min, $n = 10$, p < 0.001, Unpaired Student's t-test). Furthermore, aging axonal function was also preserved at the end of aglycemia (13%, note Fig. 4D, cyan trace, "b") followed by a remarkable recovery following aglycemia (Fig. 4E, Aging, 45.8 ± 5.5%, n = 4, 30 mM glucose versus 13.6 ± 6.6%, n = 10, 10 mM glucose, $p < 0.001$, Unpaired Student's *t*-test), which surpassed the improved recovery of young axons (Fig. 4G, comparison of fold change in pink and cyan dot plots compared to corresponding controls, Young 1.9 ± 0.2, n = 4 versus Aging 3.4 ± 0.4, n = 4, p < 0.001, One-way ANOVA followed by Newman-Keul's multiple comparison test) when incubated in 30 mM glucose before aglycemia. The consistent support of axonal function observed as a delayed reduction, preservation at the end of aglycemia, and improved extent of recovery after incubating in high glucose attest to the ability of young and aging astrocytes to upregulate their glycogen stores, convert it to lactate, and deliver it to axons for prolonged periods of time.

3.4. Substituting glucose for lactate following aglycemia identifies a metabolic switch from glucose to lactate in aging axons

We evaluated whether axons prefer lactate over glucose during recovery from aglycemia. At the end of aglycemia, MONs were superfused with ACSF containing 20 mM lactate

instead of glucose (Fig. 5). Unexpectedly, CAP area in young MONs recovered less in lactate compared to glucose following an episode of aglycemia (Fig. 5A and B, Young, 8.8 ± 6%, $n = 6$, 20 mM lactate versus 36.7 ± 13.3%, $n = 15$, 10 mM glucose, $p < 0.001$, Unpaired Student's *t*-test), while CAP area in aging MONs recovered to a similar extent in lactate or glucose (Fig. 5C and D, Aging, 9.9 ± 10%, $n = 5$, 20 mM lactate versus 13.6 ± 6.6%, $n = 10$, 10 mM glucose, $p = 0.38$, Unpaired Student's t-test). Interestingly, CAP area in young MONs recovered as little as that in aging axons when lactate was provided after aglycemia (Fig. 5E, blue, red, and brown dot plots), suggesting that a portion of young axons seems to strictly rely on glucose during recovery, while this portion of axons switches their metabolism with aging. It is important to note that lactate fails to provide post-aglycemia rescue to young or aging WM of MONs.

3.5. Lactate supports axonal function in two different WM tracts

CC is a major bundle of axons traversing between the two hemispheres and injury to CC has been implicated in many neurodegenerative diseases such as dementia, diabetes mellitus, and multiple sclerosis (Gean-Marton et al., 1991; Kodl et al., 2008; Tomimoto et al., 2004; Yamauchi et al., 2000). CC contains a mixture of myelinated and unmyelinated axons (Sturrock, 1980), as opposed to the fully myelinated axons of the optic nerve, therefore we investigated whether lactate supports myelinated and unmyelinated axon function in CC slices (Fig. 6). Typically, evoked CAPs in CC slices using extracellular recording configuration (Fig. 6A) exhibit two peaks (P); P1 for myelinated axons with a faster conduction time, and P2 for unmyelinated axons with a slower conduction time (Fig. 6B). Although aglycemia gradually suppressed the CAP area in CC slices, a portion of axons stayed functional at the end of aglycemia (Fig. 6B, Baseline, black trace; aglycemia, red trace; dotted trace, recovery; Fig. 6D, dark green time course, red arrow). Providing lactate during aglycemia fully supported axonal function (Fig. 6C, Baseline, black trace; aglycemia, red trace; dotted trace, recovery), suggesting that lactate readily substitutes for glucose in both myelinated and unmyelinated axons (Fig. 6D purple time course and 6E, purple dot plot, 101.6 ± 12.4%, n = 5, 20 mM lactate versus dark green dot plot, 43.8 ± 16%, $n = 10$, no lactate, $p < 0.001$, Unpaired Student's *t*-test). Moreover, comparing the time course of CAP area decline in MONs and CC slices revealed an unexpected resistance of CC slices to aglycemia (Fig. 6 F–H). CAP area in CC slices (Fig. 6F, dark green) fell later than CAP area in MONs (Fig. 6F, light green) and more axons subsisted functionally at the end of aglycemia (Fig. 6F, red arrow and 6H, dark green dot plot, 37.3 ± 2.4%, n = 10, CC versus light green 2.1 ± 3.2%, n = 15, MON, p < 0.001, Unpaired Student's *t*-test). Despite this resistance, CAP area recovered to a similar extent in both MONs and CC slices (Fig. 6F time courses and 6G, dot plots, light green 36.7 ± 13.3%, n = 15, MON versus dark green 47.8 ± 16%, n = 10, CC, $p = 0.31$, Unpaired Student's t-test).

3.6. Lactate supports aging CC axons

Similarly, to young CC, aglycemia suppressed the CAP area in aging slices, while a subset axons remained functional at the end of the glucose deprivation (Fig. 7A, Baseline, black trace; aglycemia, red trace; recovery, dotted trace; Fig. 7C, pink time course, red arrow). Providing lactate during aglycemia fully supported CC axon function (Fig. 7B, Baseline, black trace; aglycemia, red trace; recovery, dotted trace), suggesting that aging CC axons

effectively substitute glucose for lactate (Fig. 7C, dark pink time course and 7D, dark pink dot plot, 109.7 ± 10.5%, $n = 8$, 20 mM lactate versus light pink dot plot, 39.3 ± 6.6%, n = 8, $p < 0.0001$, unpaired Student's t-test). Furthermore, despite aging CC axons demonstrated a higher resilience to aglycemia compared to aging MON axons (Fig 7 E–G) by maintaining axon function during aglycemia (Fig. 7E–F, red arrow) and and recovering better than MON axons (Fig. 7G, light pink dot plot, CC, 24.2 ± 7.5%, $n = 6$, versus red dot plot, MON, 2.2 ± 0.5%, n = 10, p < 0.001, Unpaired Student's t-test). Moreover, young CC and aging CC comparably recovered following aglycemia (Fig. 8A, time courses, and 8B, dark green dot plot, young CC, 36.9 ± 8.5%, $n = 7$, versus light pink dot plot, aging CC, 45.0 ± 4.8%, n = 6, ns, Unpaired Student's t-test). This is in contrast to aging MON axon function which recovered poorly after aglycemia compared to young MONs (Fig. 2).

4. Discussion

The ANLS is one of the important systems providing anatomical and physiological infrastructure for glial-neuronal interactions where specialized architectural organization supports the function. However, the question arises as to whether aging astrocytes effectively take up glucose, store it as glycogen, and deliver glycogen-derived lactate to meet the needs of aging axons, and whether the ANLS is fully functional in different WM tracts such that lactate is an alternate metabolic fuel for myelinated and unmyelinated axons in different WM tracts. Our study yields a novel finding that aging astrocytes efficiently operate the ANLS; however, aging axons intrinsically become more susceptible to glucose deprivation. Moreover, lactate serves as a universal fuel to support axon function independent of age and myelin content in different WM tracts.

An intriguing finding in our study is that aging axons recovered less compared to young axons after an aglycemic episode, but they readily switched from glucose to lactate to support their function during aglycemia. Glycogen-derived lactate becomes the main fuel to support axon function when glucose is unavailable, and indeed persistence of axon function directly correlates with the extent of glycogen storage and lactate availability (Brown et al., 2003a; Tekkok et al., 2005). Consistent with this, the rate of axonal function decline and the time to complete loss of axon function in young and aging MONs were indistinguishable, suggesting similar amounts of glycogen storage in young and aging astrocytes and comparable ability of axons to use lactate as an alternative to glucose. This suggestion was further supported by the comparable amount lactate levels observed in young and aging MONs after aglycemia (Supplemental Fig. 1, A and B). The ability of lactate to support young and aging axonal function became more evident when glycogen stores in young and aging astrocytes were upregulated by incubating MONs in high glucose. Aging axons sustained their function longer, declined slower, partly remained functional at the end of aglycemia, and identically improved in recovery to young axons. Since high-glucose incubation sustained axon function in aging axons akin to young axons, this finding demonstrates that the performance of aging astrocytes to take up glucose, store it as glycogen, and convert it to lactate when glucose is absent is comparable to young astrocytes. Therefore, age-related structural reorganization of astrocytes presumably occurs to better support aging axons metabolically and aging-related alterations in WM structure are adaptations to maintain function as opposed to neurodegeneration (Baltan

et al., 2008; Stahon et al., 2016). Unfortunately, these adaptive changes in the face of a metabolic challenge (ischemia, anoxia, aglycemia) turn against and impair WM robustly, which helps to explain the underlying increased sensitivity of aging WM to injury (Baltan, 2014; Baltan et al., 2008; Stahon et al., 2016). Increased sensitivity of aging axons to glucose deprivation is yet another example. Because aging astrocytes operate the ANLS efficiently and aging axons can readily switch to lactate as an energy source, axons must become intrinsically more vulnerable to aglycemia. Potential explanations for this intrinsic vulnerability are numerous, such as structural and functional changes to axons (Baltan, 2014; Stahon et al., 2016), alterations in myelin and its composition (Peters, 2002; Peters and Sethares, 2002; Stahon et al., 2016), reorganization of mitochondrial architecture leading to functional decline, impaired smooth endoplasmic reticulum Ca+2 homeostasis, and interactions with mitochondria (Stahon et al., 2016), or age-dependent reorganization of *N*-methyl-D-aspartate (NMDA) receptors (Baltan, 2016; Baltan et al., 2011b; Stahon et al., 2016; Yang et al., 2014). Interesting evidence emerged when lactate, replacing glucose, was provided exclusively during the recovery period from aglycemia. In young MONs, recovery under these conditions prominently depressed axonal function recovery. Ironically, young axons recovered as little as aging axons when lactate replaced glucose during recovery, suggesting that axons prefer distinct metabolites during different stages of injury such that a portion of young axons was strictly dependent upon glucose during the recovery stage. In contrast, in aging MONs these glucose-dependent axons seem to already fall out of function before the recovery period since the recovery in lactate had no impact on axon function. While further experiments are currently being carried out, we suggest that aging leads to a metabolic switch in axon function-metabolite coupling affecting primarily glucose-dependent axons, leading to increased vulnerability of aging axons to aglycemia.

A further novel finding in our study is that lactate sustained axon function in CC slices, which consist of a mixture of myelinated and unmyelinated axons, indicating that lactate can equally support the function of both myelinated and unmyelinated axons in WM tracts. More importantly, CC axons displayed a greater resilience to aglycemia such that axons sustained function longer, declined slower, and a portion of axons remained functional at the end of aglycemia. On the other hand, CC axons recovered to the same extent as optic nerve axons. Axon function in CC slices is relatively more sensitive to injury compared to optic nerve (Reeves et al., 2005; Tekkok and Goldberg, 2001; Tekkok et al., 2007). For instance, exposure to transient oxygen-glucose deprivation (OGD) for 30-min results in irreversible loss of axon function in CC slices (Tekkok and Goldberg, 2001), while this duration of OGD in the optic nerve is followed by ~75% recovery (Tekkok et al., 2007). It is interesting to contemplate whether myelinated or unmyelinated axons exhibit this resilience to the removal of glucose and whether the subsequent recovery is primarily due to rescue of the function of myelinated or unmyelinated axons. Typically, evoked compound action potentials (CAPs) in CC slices exhibit two peaks, one for myelinated axons with a shorter conduction time, and a second one for unmyelinated axons with a slower conduction time. During aglycemia, the first peak showed an immediate sensitivity to glucose deprivation and disappeared first, while the remaining CAP area was mainly due to the second peak. Though the second peak also declined during aglycemia, a prominent portion was sustained, even at the end of aglycemia. Likewise, the recovery was mainly attributable to the

second peak. These observations can be interpreted as unmyelinated nerves being more resistant to aglycemia; however, it is also plausible that myelin is the immediate target, so therefore axons become demyelinated and contribute to the unmyelinated group. Further histological and ultrastructural studies are underway to conclusively answer these questions. It is important to note that there is a greater resistance of CC axons to anoxia compared to the optic nerve, suggesting that unmyelinated axons and/or the smallest axons with the thinnest myelin sheaths are resistant to anoxia (Baltan, 2006). Collectively, these results reveal that CNS WM is remarkably tolerant of glucose deprivation when lactate is available, although there is regional variability in their ability to function and survive this metabolic switch. To achieve optimal protection of the CNS in various neurological diseases, it is critical to understand the properties of regional energy metabolism and injury mechanisms for successful therapeutic approaches.

Another interesting finding is the architectural restructuring of astrocytes in WM correlated with the successful operation of the ANLS and intact NVU–astrocyte-axon function communication in aging WM. Interestingly, RNA sequencing of astrocytes from different regions of the brain across the lifespan of the mouse mice identified age-related transcriptional changes that could contribute to cognitive decline (Clarke et al., 2018). Astrocytes have distinct region-dependent transcriptomic identities and they age in a region-dependent manner. For instance, astrocytes in the hippocampus and striatum undergo more dramatic transcriptional changes compared to cortical astrocytes. As a result, aged astrocytes in the hippocampus or striatum express more reactive neuroinflammatory and ischemia-specific genes together with an activated morphology. On the other hand, the top-down regulated genes in aging astrocytes were involved in mitochondrial function, energy production, and antioxidant defense, suggesting that aging astrocytes have impaired energy capacity and low anti-oxidant ability (Clarke et al., 2018). Accordingly, age-related changes in astrocytes are increasingly accepted to underlie age-dependent alterations in the BBB, in metabolic regulation, and cognitive function. Structurally, larger GFAP (+) or S100β (+) astrocytes were observed in the aging hippocampus, specifically in the dentate gyrus (Lindsey et al., 1979). In aging WM, astrocyte cell bodies increased in size and extended larger, thicker processes following axons in a more parallel orientation, as opposed to vertical processes of young axons that interwove in and out of the axons. This configuration of astrocyte processes may serve to expand their end feet over the capillaries (Nonaka et al., 2003) to regulate glucose transport across the BBB (Andriezen, 1893; Cajal, 1909; Peters and Palay, 1991) and to better monitor function and metabolic demands of aging axons with more frequent contacts at the nodes of Ranvier (Black and Waxman, 1988). Extensive axonal energy demand and physiological maintenance of glial cells place WM tracts under metabolic challenge, under physiological conditions (Harris and Attwell, 2012; Ransom and Orkand, 1996), and with aging (Baltan, 2012; Baltan et al., 2008; Bastian et al., 2018b; Bastian et al., 2018c; Stahon et al., 2016). The unique vascular network of WM is less dense and more sparse compared to gray matter, therefore WM components and glial cells have relatively restricted access to energy substrates (Moody et al., 1990). The design of oligodendrocytes wrapping myelin around axons to facilitate axon transport also inevitably forms a barrier and restricts extracellular metabolites from gaining access to axons (Nave, 2010a, 2010b). Aging axons reorganize their myelin and myelin content as well as their

nodal and internodal distances (Stahon et al., 2016); therefore, it is not surprising that astrocytes conform and accommodate these changes to properly nourish aging axons.

Brain energy metabolism is interrupted in many neurological disorders. Energy failure is the central cause of loss of cerebral function during a hypoglycemic attack or in diseases such as diabetes mellitus (DM). Astrocytes in WM store glycogen that is converted to lactate when glucose concentration is low or when there is increased energy demand, confirming that CNS WM glycogen plays a crucial role as an energy reserve and buffer store (Brown et al., 2003a; Brown et al., 2005; Ransom and Fern, 1997; Wender et al., 2000). Glycogen content present in the tissue at the onset of aglycemia determines the duration of axonal function (Brown et al., 2003a; Brown et al., 2005; Ransom and Fern, 1997; Wender et al., 2000), a relationship that may have profound implications for patients that suffer from Type-1 DM and experience frequent silent WM infarcts leading to declining cognitive function. Similarly, axon function as the presynaptic input dictates synaptic transmission and synaptic plasticity underlying learning and memory-related events that decline with age and in neurodegenerative diseases. Therefore, all evidence points toward astrocyte-derived lactate as a crucial substrate, and this metabolic coupling is validated in both gray matter and WM portions of the brain. Astrocytes transporting glucose from the vascular end to neuronal and glial cells also highlight an important mission of the NVU. Oligodendrocytes, microglia, vascular cells consisting of endothelial cells, smooth muscle cells, pericytes, and ECM, and astrocytes form a complex and intricate arrangement. The dynamic interaction among each component within the NVU contributes to the clinical outcome of numerous CNS diseases. Subsequently, modulation of the astrocyte-neuron lactate shuttle system may be important in developing therapies for neurodegenerative diseases (Yamagata, 2022). For instance, defects in ANLS in in vivo and in vitro models of AD have been reported (Sun et al., 2020). Administration of fibroblast growth factor 21 (FGF21) improves memory, attenuates amyloid deposition and tau phosphorylation by regulating in part MCTs. It is proposed that the neuroprotective effects of FGF21 are due to its central effects on energy metabolism and ANLS. Interestingly, ANLS performance has the capacity to be modified, even in the adult brain, by simply altering lifestyle such as diet (Leino et al., 2001). Switching to a ketogenic diet can upregulate MCT1 levels by eight-fold on abluminal endothelial membranes as well as increasing glucose transporter (GLUT1) readjusting choice of fuel for brain. The regulation of MCT1 by ketogenic diet may have important implications under stress conditions such as epilepsy. Increasing astrocytic lactate production by upregulating MCT levels is also proposed as a potential therapeutic strategy to improve recovery after stroke (Yamagata, 2022). In addition to its importance in the field of stroke, NVU dysfunction is now accepted as a cause or a result of other CNS diseases including Alzheimer’s disease, vascular dementia, Parkinson’s disease, amyotrophic lateral sclerosis, and multiple sclerosis (Arai et al., 2011). Furthermore, the components represent heterogeneity in their morphology, developmental origin, and physiological properties and function while they respond to injury, maintaining their interaction with each other. Therefore ANLS is an important part of the cell-cell signaling mechanism that contributes to multi-complex functions of the NVU under physiological and pathological conditions.

Supplementary Material

Refer to Web version on PubMed Central for supplementary material.

Acknowledgments

We thank Ngoc Wasson, MPH, Technical Writer, Anesthesiology & Perioperative Medicine, OHSU, for editing this manuscript.

Funding

This study was supported by the NIH NINDS (1R21NS094881) and NIA (AG033720).

Abbreviations:

ACSF	artificial cerebrospinal fluid
ANLS	astrocyte-neuron lactate shuttle
AOI	areas of interest
BBB	blood-brain barrier
CAP	compound action potential
CC	corpus callosum
CNS	central nervous system
DM	diabetes mellitus
ECM	extracellular matrix
GFAP	glial fibrillary acidic protein
GLUT 1	glucose transporter 1
IHC	immunohistochemistry
MCT	monocarboxylate transporter
MONs	mouse optic nerves
NMDA	*N*-methyl-D-aspartate
NVU	neurovascular unit
OGD	oxygen-glucose deprivation
WM.	white matter.

References

Adijanto J, Philp NJ, 2012. The SLC16A family of monocarboxylate transporters (MCTs)–physiology and function in cellular metabolism, pH homeostasis, and fluid transport. Curr. Top. Membr 70, 275–311. [PubMed: 23177990]

Amaral AI, Teixeira AP, Sonnewald U, Alves PM, 2011. Estimation of intracellular fluxes in cerebellar neurons after hypoglycemia: importance of the pyruvate recycling pathway and glutamine oxidation. J. Neurosci. Res 89, 700–710. [PubMed: 21337365]

Andriezen WL, 1893. The neuroglia elements in the human brain. Br. Med. J 2, 227–230.

Arai K, Lok J, Guo S, Hayakawa K, Xing C, Lo EH, 2011. Cellular mechanisms of neurovascular damage and repair after stroke. J. Child Neurol 26, 1193–1198. [PubMed: 21628695]

Baltan S, 2006. Surviving anoxia: a tale of two white matter tracts. Crit. Rev. Neurobiol 18, 95–103. [PubMed: 17725512]

Baltan S, 2012. Histone deacetylase inhibitors preserve function in aging axons. J. Neurochem 123 (Suppl. 2), 108–115. [PubMed: 23050648]

Baltan S, 2014. Excitotoxicity and mitochondrial dysfunction underlie age-dependent ischemic white matter injury. Adv Neurobiol 11, 151–170. [PubMed: 25236728]

Baltan S, 2016. Age-specific localization of NMDA receptors on oligodendrocytes dictates axon function recovery after ischemia. Neuropharmacology 110, 626–632. [PubMed: 26407763]

Baltan S, Besancon EF, Mbow B, Ye Z, Hamner MA, Ransom BR, 2008. White matter vulnerability to ischemic injury increases with age because of enhanced excitotoxicity. J. Neurosci 28, 1479–1489. [PubMed: 18256269]

Baltan S, Bachleda A, Morrison RS, Murphy SP, 2011a. Expression of histone deacetylases in cellular compartments of the mouse brain and the effects of ischemia. Transl. Stroke Res 2, 411–423. [PubMed: 21966324]

Baltan S, Murphy SP, Danilov CA, Bachleda A, Morrison RS, 2011b. Histone deacetylase inhibitors preserve white matter structure and function during ischemia by conserving ATP and reducing excitotoxicity. J. Neurosci 31, 3990–3999. [PubMed: 21411642]

Baltan S, Morrison RS, Murphy SP, 2013. Novel protective effects of histone deacetylase inhibition on stroke and white matter ischemic injury. Neurotherapeutics 10, 798–807. [PubMed: 23881453]

Baltan S, Bastian C, Quinn J, Aquila D, McCray A, Brunet S, 2018. CK2 inhibition protects white matter from ischemic injury. Neurosci. Lett 687, 37–42. [PubMed: 30125643]

Bastian C, Politano S, Day J, McCray A, Brunet S, Baltan S, 2018a. Mitochondrial dynamics and preconditioning in white matter. Cond Med 1, 64–72. [PubMed: 30135960]

Bastian C, Quinn J, Tripathi A, Aquila D, McCray A, Dutta R, Baltan S, Brunet S, 2018b. CK2 inhibition confers functional protection to young and aging axons against ischemia by differentially regulating the CDK5 and AKT signaling pathways. Neurobiol. Dis 126, 47–61. [PubMed: 29944965]

Bastian C, Zaleski J, Stahon K, Parr B, McCray A, Day J, Brunet S, Baltan S, 2018c. NOS3 inhibition confers post-ischemic protection to young and aging white matter integrity by conserving mitochondrial dynamics and miro-2 levels. J. Neurosci 38, 6247–6266. [PubMed: 29891729]

Bastian C, Quinn J, Doherty C, Franke C, Faris A, Brunet S, Baltan S, 2019. Role of brain glycogen during ischemia, aging and cell-to-cell interactions. Adv Neurobiol 23, 347–361. [PubMed: 31667815]

Bergersen LH, 2015. Lactate transport and signaling in the brain: potential therapeutic targets and roles in body-brain interaction. J. Cereb. Blood Flow Metab 35, 176–185. [PubMed: 25425080]

Berkich DA, Ola MS, Cole J, Sweatt AJ, Hutson SM, LaNoue KF, 2007. Mitochondrial transport proteins of the brain. J. Neurosci. Res 85, 3367–3377. [PubMed: 17847082]

Black JA, Waxman SG, 1988. The perinodal astrocyte. Glia 1, 169–183. [PubMed: 2976037]

Bolanos JP, Almeida A, Moncada S, 2010. Glycolysis: a bioenergetic or a survival pathway? Trends Biochem. Sci 35, 145–149. [PubMed: 20006513]

Bouzier-Sore AK, Voisin P, Bouchaud V, Bezancon E, Franconi JM, Pellerin L, 2006. Competition between glucose and lactate as oxidative energy substrates in both neurons and astrocytes: a comparative NMR study. Eur. J. Neurosci 24, 1687–1694. [PubMed: 17004932]

Broer S, Rahman B, Pellegri G, Pellerin L, Martin JL, Verleysdonk S, Hamprecht B, Magistretti PJ, 1997. Comparison of lactate transport in astroglial cells and monocarboxylate transporter 1 (MCT 1) expressing Xenopus laevis oocytes. Expression of two different monocarboxylate transporters in astroglial cells and neurons. J. Biol. Chem 272, 30096–30102. [PubMed: 9374487]

Brown AM, Baltan Tekkök S, Ransom BR, 2003a. Glycogen regulation and functional role in mouse white matter. J. Physiol 549 (2), 501–512. [PubMed: 12679378]

Brown AM, Tekkok SB, Ransom BR, 2003b. Glycogen regulation and functional role in mouse white matter. J. Physiol 549, 501–512. [PubMed: 12679378]

Brown AM, Sickmann HM, Fosgerau K, Lund TM, Schousboe A, Waagepetersen HS, Ransom BR, 2005. Astrocyte glycogen metabolism is required for neural activity during aglycemia or intense stimulation in mouse white matter. J. Neurosci. Res 79, 74–80. [PubMed: 15578727]

Bushong EA, Martone ME, Ellisman MH, 2004. Maturation of astrocyte morphology and the establishment of astrocyte domains during postnatal hippocampal development. Int. J. Dev. Neurosci 22, 73–86. [PubMed: 15036382]

Cajal SR, 1909. Histologie du système nerveux. A. Maloine 1909–1911.

Cataldo AM, Broadwell RD, 1986. Cytochemical identification of cerebral glycogen and glucose-6-phosphatase activity under normal and experimental conditions: I. neurons and glia. J. Electron Microscopy Techn 3, 413–437.

Cavallotti C, Pacella E, Pescosolido N, Tranquilli-Leali FM, Feher J, 2002. Age-related changes in the human optic nerve. Can. J. Ophthalmol 37, 389–394. [PubMed: 12516719]

Cavallotti C, Cavallotti D, Pescosolido N, Pacella E, 2003. Age-related changes in rat optic nerve: morphological studies. Anat. Histol. Embryol 32, 12–16. [PubMed: 12733267]

Clarke LE, Liddelow SA, Chakraborty C, Munch AE, Heiman M, Barres BA, 2018. Normal aging induces A1-like astrocyte reactivity. Proc. Natl. Acad. Sci. U. S. A 115, E1896–E1905. [PubMed: 29437957]

Deitmer JW, Theparambil SM, Ruminot I, Noor SI, Becker HM, 2019. Energy dynamics in the brain: contributions of astrocytes to metabolism and pH homeostasis. Front. Neurosci 13, 1301. [PubMed: 31866811]

Dringen R, Hamprecht B, 1993. Differences in glycogen metabolism in astroglia-rich primary cultures and sorbitol-selected astroglial cultures derived from mouse brain. Glia 8, 143–149. [PubMed: 8225556]

Fabricius K, Jacobsen JS, Pakkenberg B, 2013. Effect of age on neocortical brain cells in 90+ year old human females–a cell counting study. Neurobiol. Aging 34, 91–99. [PubMed: 22878165]

Ferguson BS, Rogatzki MJ, Goodwin ML, Kane DA, Rightmire Z, Gladden LB, 2018. Lactate metabolism: historical context, prior misinterpretations, and current understanding. Eur. J. Appl. Physiol 118, 691–728. [PubMed: 29322250]

Foster RE, Connors BW, Waxman SG, 1982. Rat optic nerve: electrophysiological, pharmacological and anatomical studies during development. Brain Res 255, 371–386. [PubMed: 7066695]

Gean-Marton AD, Vezina LG, Marton KI, Stimac GK, Peyster RG, Taveras JM, Davis KR, 1991. Abnormal corpus callosum: a sensitive and specific indicator of multiple sclerosis. Radiology 180, 215–221. [PubMed: 2052698]

Halim ND, McFate T, Mohyeldin A, Okagaki P, Korotchkina LG, Patel MS, Jeoung NH, Harris RA, Schell MJ, Verma A, 2010. Phosphorylation status of pyruvate dehydrogenase distinguishes metabolic phenotypes of cultured rat brain astrocytes and neurons. Glia 58, 1168–1176. [PubMed: 20544852]

Harris JJ, Attwell D, 2012. The energetics of CNS white matter. J. Neurosci 32, 356–371. [PubMed: 22219296]

Herrero-Mendez A, Almeida A, Fernández E, Maestre C, Moncada S, Bolaños JP, 2009. The bioenergetic and antioxidant status of neurons is controlled by continuous degradation of a key glycolytic enzyme by APC/C–Cdh1. Nat. Cell Biol 11, 747. [PubMed: 19448625]

Itoh Y, Esaki T, Shimoji K, Cook M, Law MJ, Kaufman E, Sokoloff L, 2003. Dichloroacetate effects on glucose and lactate oxidation by neurons and astroglia in vitro and on glucose utilization by brain in vivo. Proc. Natl. Acad. Sci. U. S. A 100, 4879–4884. [PubMed: 12668764]

Kodl CT, Franc DT, Rao JP, Anderson FS, Thomas W, Mueller BA, Lim KO, Seaquist ER, 2008. Diffusion tensor imaging (DTI) identifies deficits in white matter microstructure in subjects with type 1 diabetes mellitus that correlate with reduced neurocognitive function. Diabetes. 57 (11), 3083–3089. [PubMed: 18694971]

Leino RL, Gerhart DZ, Duelli R, Enerson BE, Drewes LR, 2001. Diet-induced ketosis increases monocarboxylate transporter (MCT1) levels in rat brain. Neurochem. Int 38, 519–527. [PubMed: 11248400]

Lindsey JD, Landfield PW, Lynch G, 1979. Early onset and topographical distribution of hypertrophied astrocytes in hippocampus of aging rats: a quantitative study. J. Gerontol 34, 661–671. [PubMed: 469184]

Magistretti PJ, Sorg O, Yu N, Martin JL, Pellerin L, 1993. Neurotransmitters regulate energy metabolism in astrocytes: implications for the metabolic trafficking between neural cells. Dev. Neurosci 15, 306–312. [PubMed: 7805583]

Magistretti PJ, Sorg O, Naichen Y, Pellerin L, de Rham S, Martin JL, 1994. Regulation of astrocyte energy metabolism by neurotransmitters. Ren. Physiol. Biochem 17, 168–171. [PubMed: 7518950]

Moody DM, Bell MA, Challa VR, 1990. Features of the cerebral vascular pattern that predict vulnerability to perfusion or oxygenation deficiency: an anatomic study. AJNR Am. J. Neuroradiol 11, 431–439. [PubMed: 2112304]

Murphy SP, Lee RJ, McClean ME, Pemberton HE, Uo T, Morrison RS, Bastian C, Baltan S, 2014. MS-275, a class I histone deacetylase inhibitor, protects the p53-deficient mouse against ischemic injury. J. Neurochem 129, 509–515. [PubMed: 24147654]

Nave KA, 2010a. Myelination and the trophic support of long axons. Nat. Rev. Neurosci 11, 275–283. [PubMed: 20216548]

Nave KA, 2010b. Oligodendrocytes and the “micro brake” of progenitor cell proliferation. Neuron 65, 577–579. [PubMed: 20223193]

Nave KA, Ehrenreich H, 2014. Myelination and oligodendrocyte functions in psychiatric diseases. JAMA Psychiatry 71, 582–584. [PubMed: 24671770]

Nonaka H, Akima M, Hatori T, Nagayama T, Zhang Z, Ihara F, 2003. Microvasculature of the human cerebral white matter: arteries of the deep white matter. Neuropathology 23, 111–118. [PubMed: 12777099]

Pellegri G, Rossier C, Magistretti PJ, Martin JL, 1996. Cloning, localization and induction of mouse brain glycogen synthase. Brain Res. Mol. Brain Res 38, 191–199. [PubMed: 8793107]

Pellerin L, Pellegri G, Martin JL, Magistretti PJ, 1998. Expression of monocarboxylate transporter mRNAs in mouse brain: support for a distinct role of lactate as an energy substrate for the neonatal vs. adult brain. Proc. Natl. Acad. Sci. U. S. A 95, 3990–3995. [PubMed: 9520480]

Peters A, 2002. The effects of normal aging on myelin and nerve fibers: a review. J. Neurocytol 31, 581–593. [PubMed: 14501200]

Peters A, Palay S, 1991. Webster H. de F. (1991) The Fine Structure of the Nervous System. Neurons and their Supporting Cells. New York, Oxford.

Peters A, Sethares C, 2002. Aging and the myelinated fibers in prefrontal cortex and corpus callosum of the monkey. J. Comp. Neurol 442, 277–291. [PubMed: 11774342]

Pfeiffer-Guglielmi B, Fleckenstein B, Jung G, Hamprecht B, 2003. Immunocytochemical localization of glycogen phosphorylase isozymes in rat nervous tissues by using isozyme-specific antibodies. J. Neurochem 85, 73–81. [PubMed: 12641728]

Poole RC, Sansom CE, Halestrap AP, 1996. Studies of the membrane topology of the rat erythrocyte H+/lactate cotransporter (MCT1). Biochem. J 320 (Pt 3), 817–824. [PubMed: 9003367]

Ramos KL, Colquhoun A, 2003. Protective role of glucose-6-phosphate dehydrogenase activity in the metabolic response of C6 rat glioma cells to polyunsaturated fatty acid exposure. Glia 43, 149–166. [PubMed: 12838507]

Ransom BR, Fern R, 1997. Does astrocytic glycogen benefit axon function and survival in CNS white matter during glucose deprivation? Glia 21, 134–141. [PubMed: 9298856]

Ransom BR, Orkand RK, 1996. Glial-neuronal interactions in non-synaptic areas of the brain: studies in the optic nerve. Trends Neurosci 19, 352–358. [PubMed: 8843605]

Reeves TM, Phillips LL, Povlishock JT, 2005. Myelinated and unmyelinated axons of the corpus callosum differ in vulnerability and functional recovery following traumatic brain injury. Exp. Neurol 196, 126–137. [PubMed: 16109409]

Saab AS, Tzvetavona ID, Trevisiol A, Baltan S, Dibaj P, Kusch K, Mobius W, Goetze B, Jahn HM, Huang W, Steffens H, Schomburg ED, Perez-Samartin A, Perez-Cerda F, Bakhtiari D, Matute

C, Lowel S, Griesinger C, Hirrlinger J, Kirchhoff F, Nave KA, 2016. Oligodendroglial NMDA receptors regulate glucose import and axonal energy metabolism. Neuron 91, 119–132. [PubMed: 27292539]

Sanchez-Abarca LI, Tabernero A, Medina JM, 2001. Oligodendrocytes use lactate as a source of energy and as a precursor of lipids. Glia 36, 321–329. [PubMed: 11746769]

Schurr A, West CA, Rigor BM, 1988. Lactate-supported synaptic function in the rat hippocampal slice preparation. Science 240, 1326–1328. [PubMed: 3375817]

Stahon KE, Bastian C, Griffith S, Kidd GJ, Brunet S, Baltan S, 2016. Age-related changes in axonal and mitochondrial ultrastructure and function in white matter. J. Neurosci 36, 9990–10001. [PubMed: 27683897]

Sturrock R, 1980. Myelination of the mouse corpus callosum. Neuropathol. Appl. Neurobiol 6, 415–420. [PubMed: 7453945]

Sun Y, Wang Y, Chen ST, Chen YJ, Shen J, Yao WB, Gao XD, Chen S, 2020. Modulation of the astrocyte-neuron lactate shuttle system contributes to neuroprotective action of fibroblast growth factor 21. Theranostics 10, 8430–8445. [PubMed: 32724479]

Tekkok SB, Goldberg MP, 2001. Ampa/kainate receptor activation mediates hypoxic oligodendrocyte death and axonal injury in cerebral white matter. J. Neurosci 21, 4237–4248. [PubMed: 11404409]

Tekkok SB, Ransom BR, 2004. Anoxia effects on CNS function and survival: regional differences. Neurochem. Res 29, 2163–2169. [PubMed: 15662851]

Tekkok SB, Brown AM, Westenbroek R, Pellerin L, Ransom BR, 2005. Transfer of glycogen-derived lactate from astrocytes to axons via specific monocarboxylate transporters supports mouse optic nerve activity. J. Neurosci. Res 81, 644–652. [PubMed: 16015619]

Tekkok SB, Ye Z, Ransom BR, 2007. Excitotoxic mechanisms of ischemic injury in myelinated white matter. J. Cereb. Blood Flow Metab 27, 1540–1552. [PubMed: 17299453]

Tomimoto H, Lin JX, Matsuo A, Ihara M, Ohtani R, Shibata M, Miki Y, Shibasaki H, 2004. Different mechanisms of corpus callosum atrophy in Alzheimer's disease and vascular dementia. J. Neurol 251, 398–406. [PubMed: 15083283]

Walz W, Mukerji S, 1988. Lactate release from cultured astrocytes and neurons: a comparison. Glia 1, 366–370. [PubMed: 2976396]

Wender R, Brown AM, Fern R, Swanson RA, Farrell K, Ransom BR, 2000. Astrocytic glycogen influences axon function and survival during glucose deprivation in central white matter. J. Neurosci 20, 6804–6810. [PubMed: 10995824]

Yamagata K, 2022. Lactate supply from astrocytes to neurons and its role in ischemic stroke-induced neurodegeneration. Neuroscience 481, 219–231. [PubMed: 34843897]

Yamauchi H, Fukuyama H, Nagahama Y, Katsumi Y, Hayashi T, Oyanagi C, Konishi J, Shio H, 2000. Comparison of the pattern of atrophy of the corpus callosum in frontotemporal dementia, progressive supranuclear palsy, and Alzheimer's disease. J. Neurol. Neurosurg. Psychiatry 69, 623–629. [PubMed: 11032614]

Yang X, Hamner MA, Brown AM, Evans RD, Ye ZC, Chen S, Ransom BR, 2014. Novel hypoglycemic injury mechanism: N-methyl-D-aspartate receptor–mediated white matter damage. Ann. Neurol 75, 492–507. [PubMed: 24242287]

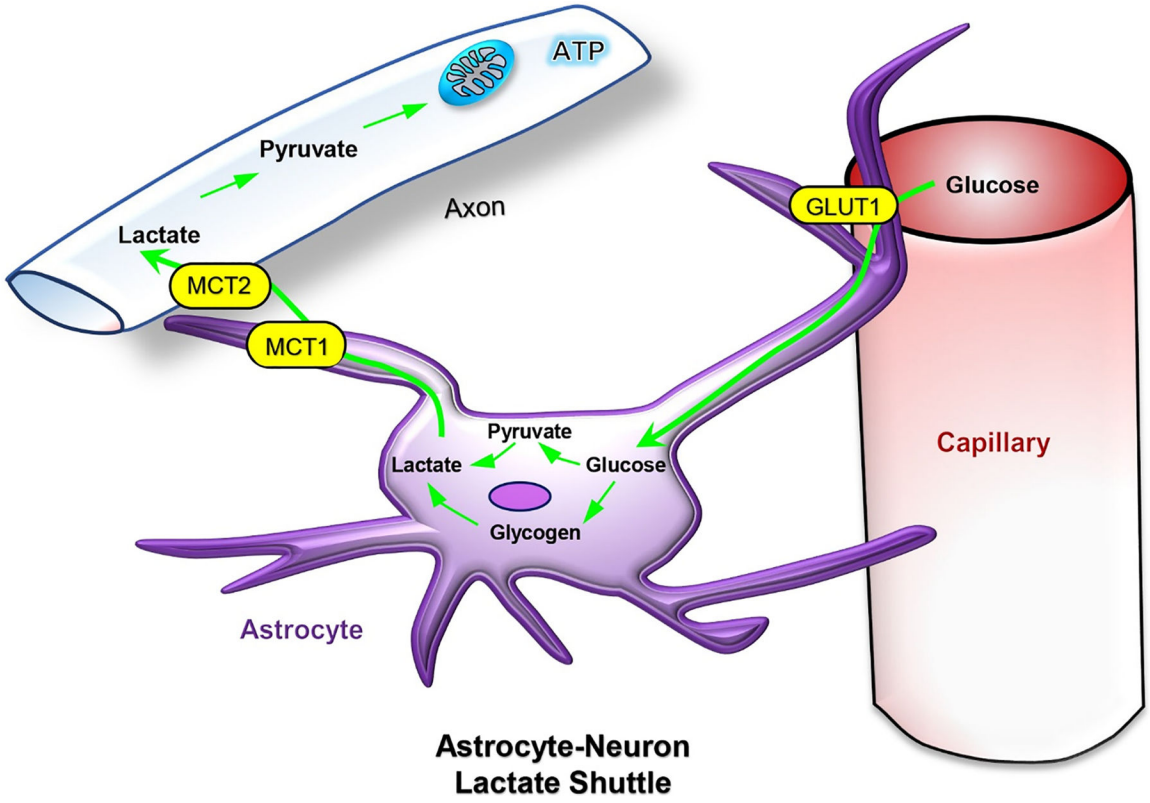

Fig. 1. The Astrocyte-Neuron Lactate Shuttle (ANLS) provides the main supply for axonal energy metabolism.

This simplified schematic displays the shuttle of lactate from astrocytes to axons. Astrocytes form a barrier between blood and axons. Astrocytes possess glycogen stores that are metabolized to lactate and serve as a main source of nutrients for axonal metabolism. The glucose-lactate exchange is achieved through a system of GLUTs (glucose transporters) and MCTs (monocarboxylate transporters). (Bastian et al., 2019).

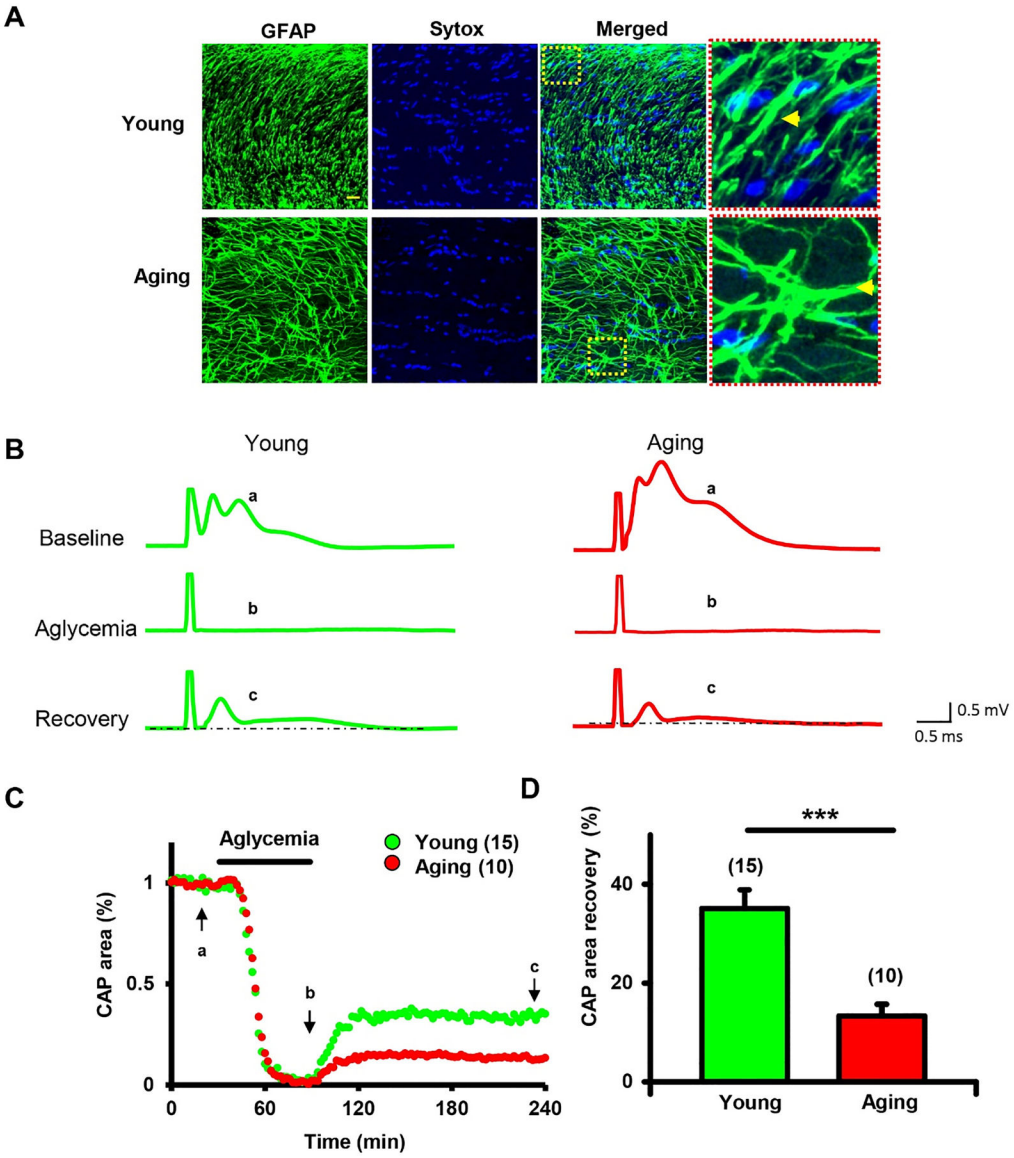

Fig. 2. Aging WM is highly vulnerable to aglycemia.

A) GFAP (+) astrocytes in young mouse optic nerves are smaller with vertically running processes, whereas aging white matter shows thicker process that are arranged parallel to axons. Yellow dashed rectangles in merged images are shown as a close-up in the far-right column. Note yellow arrow heads indicate axon run direction. **B**) Representative CAP traces from young (green) and aging (red) MONs under baseline, aglycemia, and recovery conditions. **C**) Time course shows loss of axon function in young (green) and aging (red) axons following aglycemia. In B, representative traces from baseline (a), aglycemia (b), and recovery (c) conditions, chosen are at indicated time points by arrows in C. **D**) Aging axons show impaired recovery following aglycemia when compared to young axons. *** $p < 0.001$, unpaired Student's two-tailed *t*-test.(Bastian et al., 2019). (For interpretation of the references to colour in this figure legend, the reader is referred to the web version of this article.)

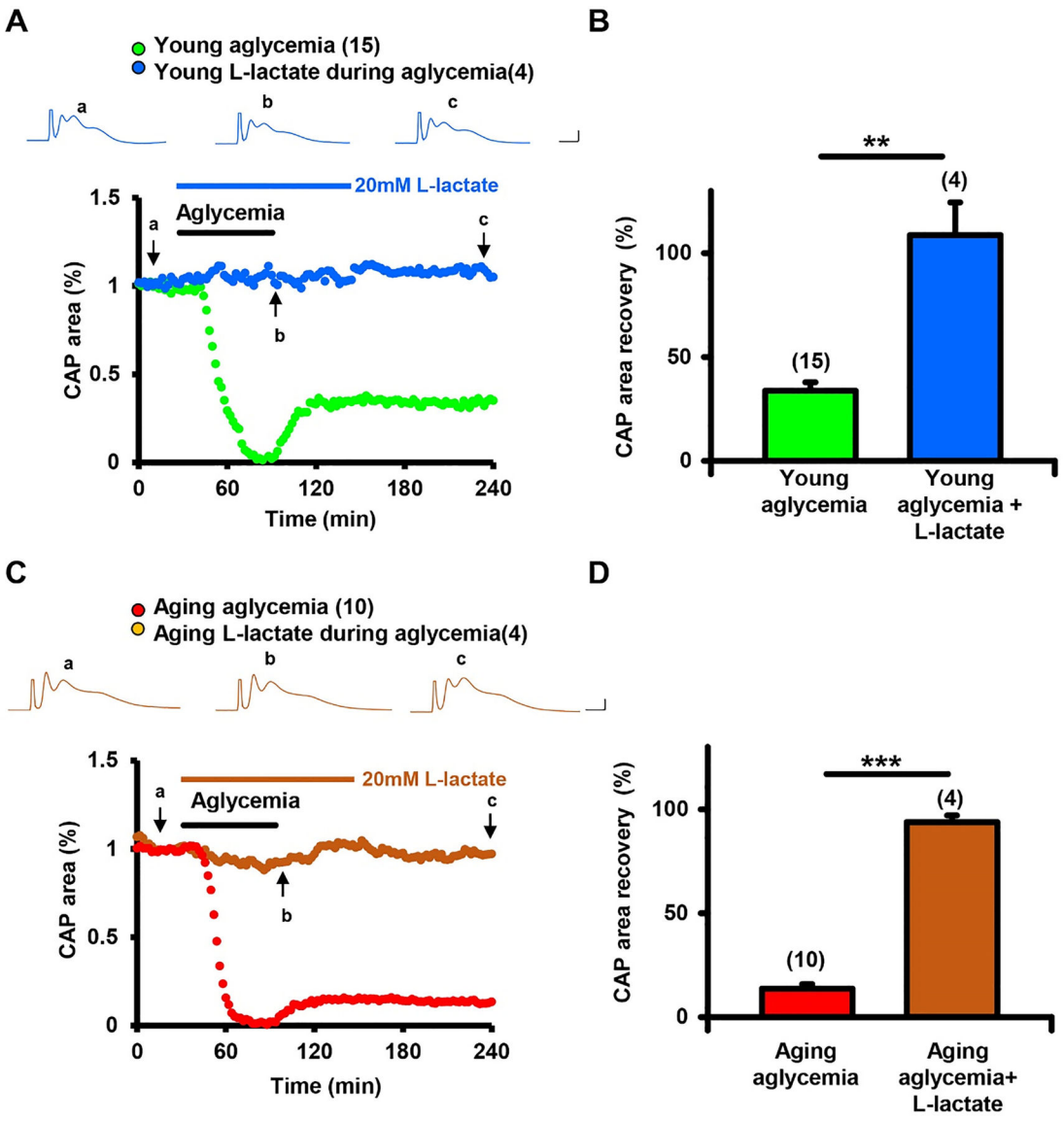

Fig. 3. L-lactate application during aglycemia prevents axon injury in both young and aging WM.

Time course of CAP Area (**A** and **C**) and CAP area recovery at 2 h after aglycemia (**B** and **D**) shows that L-lactate application during aglycemia (blue, young, vs. brown, aging) preserved axonal function and protected against aglycemic injury in MONs. Inset shows CAP traces from baseline (a), aglycemia (b), and recovery (c) conditions, which are indicated by arrows in graphs *** $p < 0.001$, unpaired Student's two-tailed *t*-test. (For interpretation of the references to colour in this figure legend, the reader is referred to the web version of this article.)

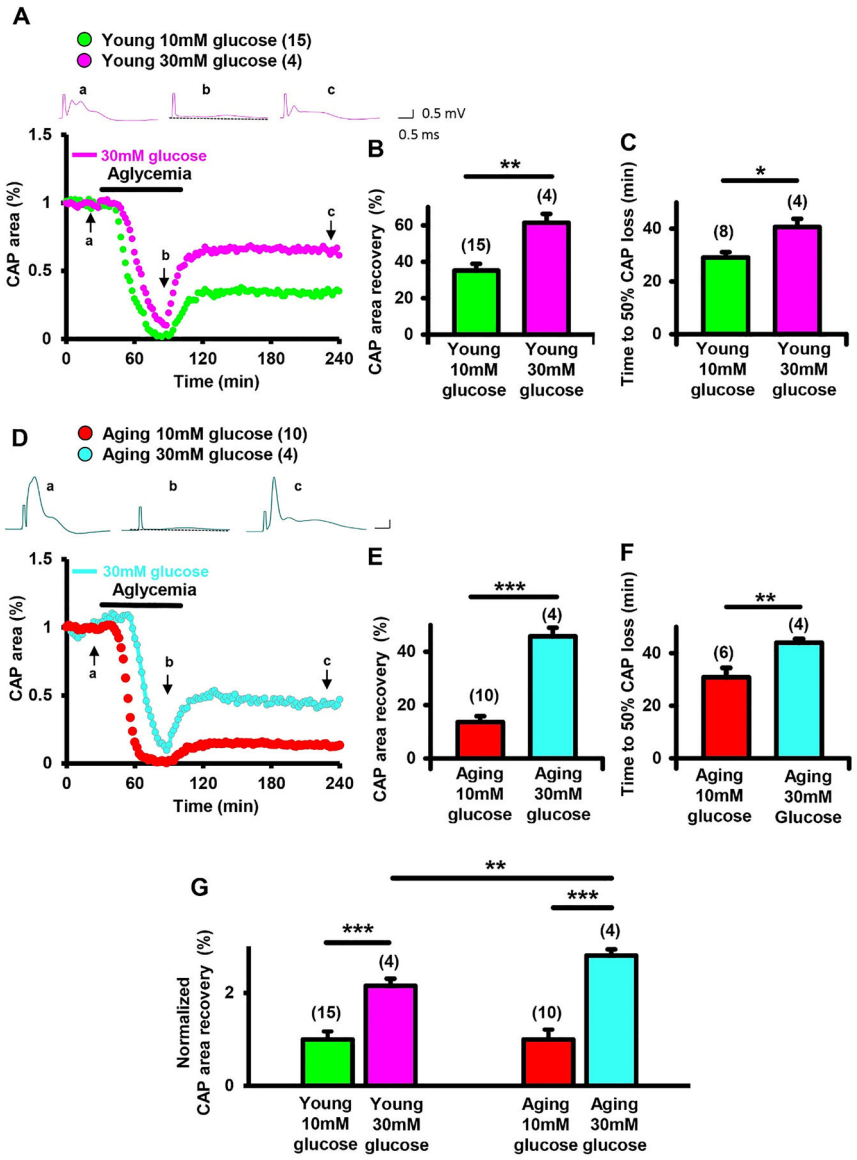

Fig. 4. High-glucose pre-incubation improves axonal function in both young and aging aglycemic WM.

Inset shows CAP traces from baseline (a), aglycemia (b), and recovery (c) conditions. High glucose (30 mM) incubation improved axon function recovery in both young (pink, **A-C**) and aging (cyan, **D-F**) WM compared to aglycemia alone (green, young; red, aging). (C) and (D) High-glucose incubation improved axon function and delays functional loss during aglycemia (b) in both young and aging MONs. (G) Interestingly, aging axons utilized lactate more efficiently during aglycemia compared to young axons. * $p < 0.05$ ** $p < 0.01$ *** $p < 0.001$, Unpaired Student two-tailed t-test (**B**, **C**, **E**, **F**) and one-way ANOVA with Newman-Keuls post hoc test (**G**). (For interpretation of the references to colour in this figure legend, the reader is referred to the web version of this article.)

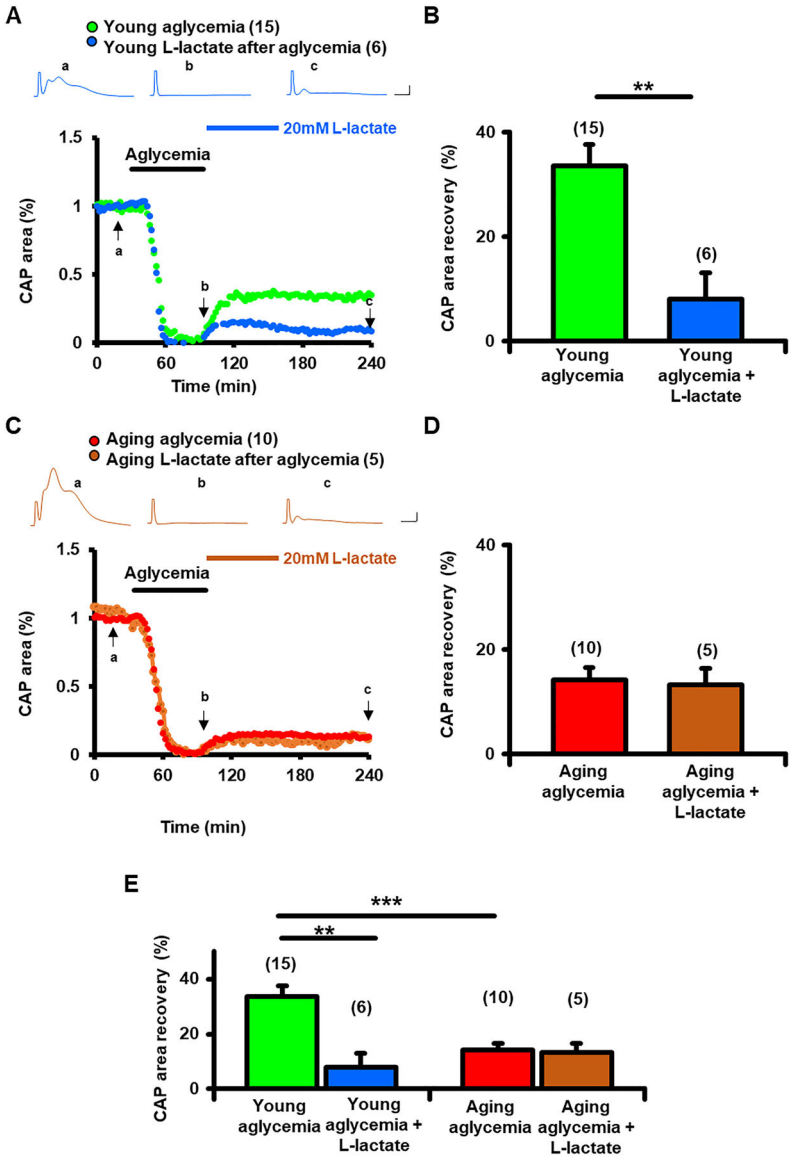

Fig. 5. L-lactate application after aglycemia identifies a metabolic switch from glucose to lactate in aging axons.

(**A**) and (**B**) In young MONs, CAP area following post-aglycemia application of L-lactate (blue) in young MONs recovered less compared to glucose (green) suggesting a subgroup of young axons preferentially metabolize glucose during recovery period. (**C**) and (**D**) On the other hand, L-lactate post-aglycemia application (brown) did not show any changes in axonal function recovery in aging MONs when compared to glucose (red) suggesting loss of subgroup of glucose preferring axons with age.

(**E**) Axonal function recovery in young MONs was comparable to that of aging axons when lactate was provided after aglycemia. Lactate supplementation post-aglycemia unmasked a metabolic switch and loss of a subset of axons using glucose during recovery with aging. ** $p < 0.01$ *** $p < 0.001$, unpaired Student two-tailed *t*-test (**B, D**) and one-way ANOVA with Newman-Keuls post hoc test (**E**). (For interpretation of the references to colour in this figure legend, the reader is referred to the web version of this article.)

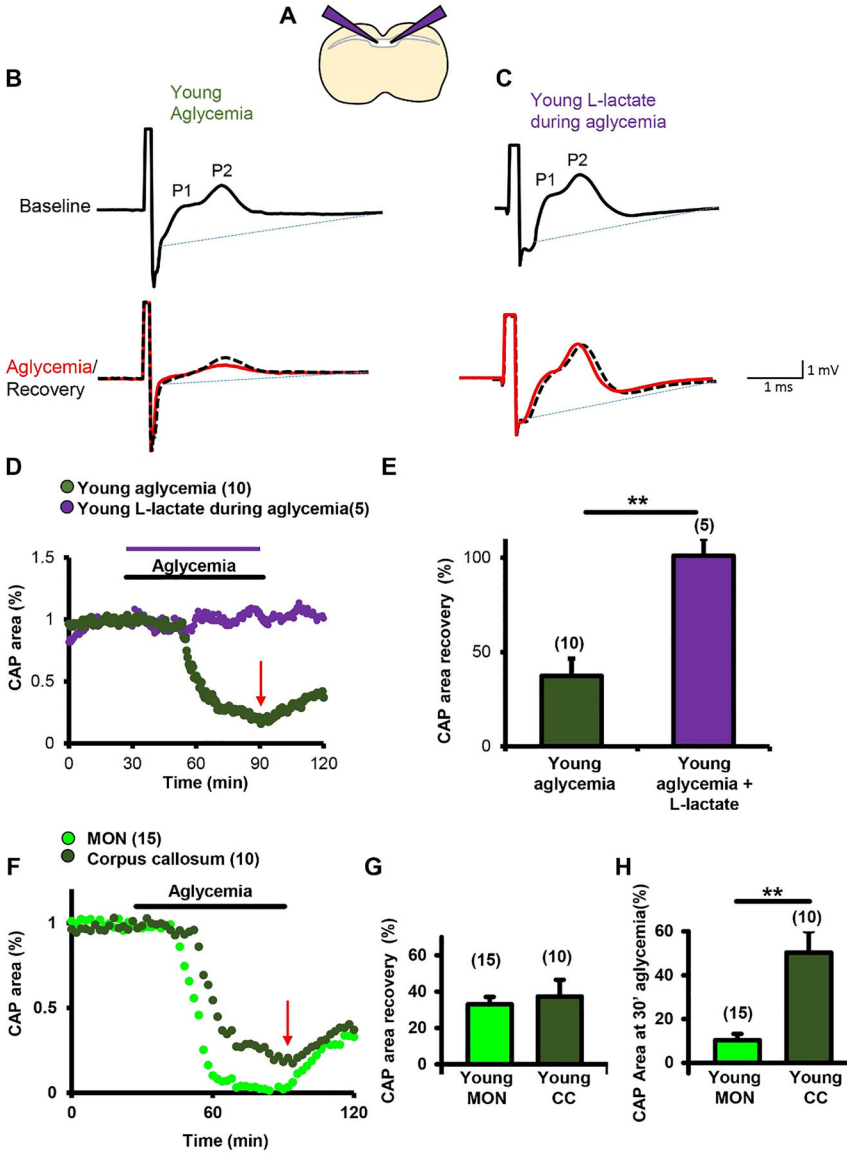

Fig. 6. Lactate is as effective as glucose in supporting corpus callosum function.

(**A**) A schematic showing a coronal section of the mouse brain and the site of placement of sharp electrodes for corpus callosum CAP recordings. CAP traces are from baseline (black), aglycemia (red), and recovery (dotted black) conditions with aglycemia (left, **B**) and L-lactate application during aglycemia (right, **C**). Note that P1 representing myelinated axons and P2 representing unmyelinated axons are the two peaks observed in CC CAP recordings. CAP area is quantified by measuring the area above the blue dotted lines and the response. (**D** and **E**) Application of L-lactate (purple) during aglycemia in young CC preserved axonal function when compared to glucose (dark green). (**F**) Time course displays CAP area changes when young MON (light green) and young CC (dark green) were exposed to 1 h of aglycemia. (**G**) CAP area recovery was comparable in both MONs and CC. (**H**) During aglycemia, CC axons were more resilient than MON axons. CAP area from CC slices at end of aglycemia (red arrow, **D** and **F**) was higher when compared to MONs. ***

$p < 0.001$, unpaired Student's two-tailed t-test. (For interpretation of the references to colour in this figure legend, the reader is referred to the web version of this article.)

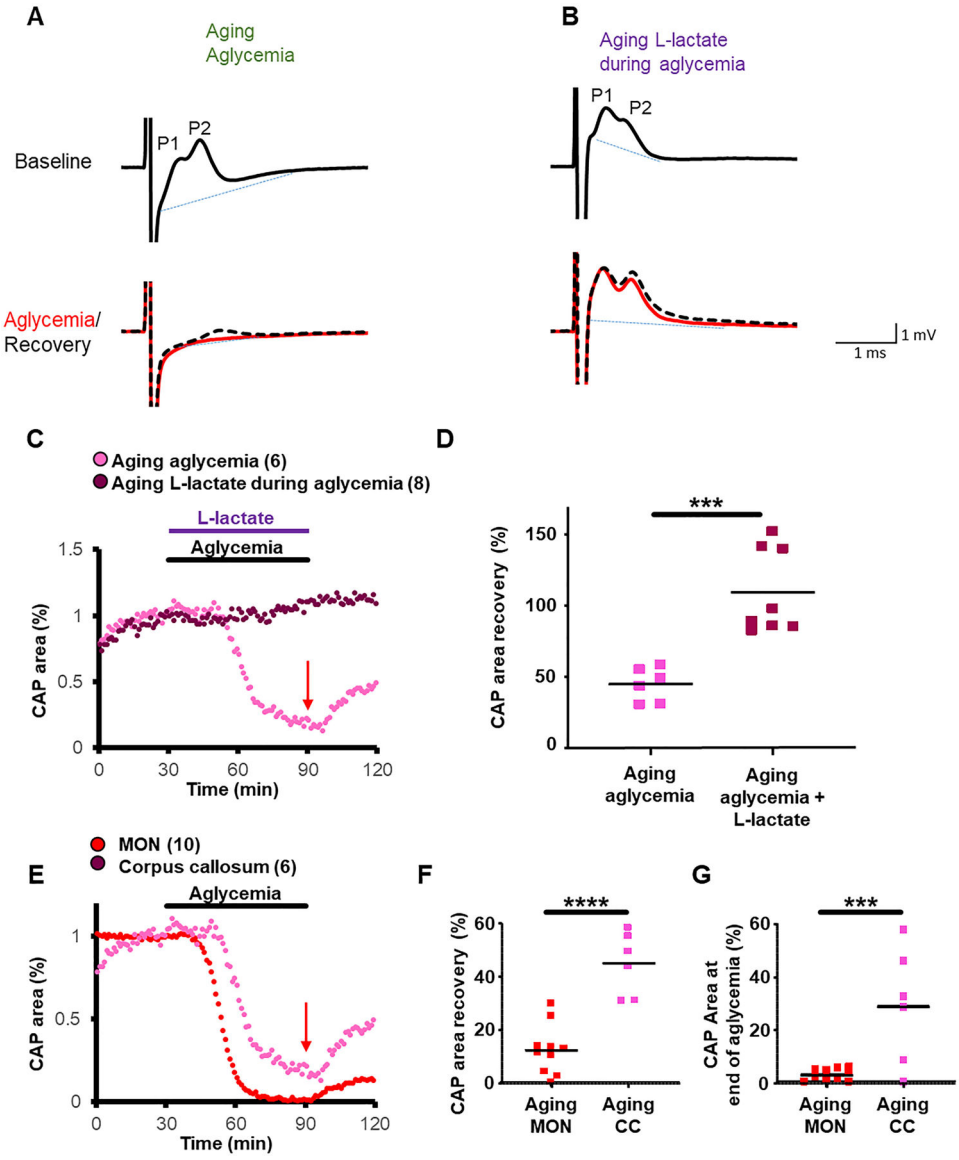

Fig. 7. Lactate efficiently supports aging corpus callosum function.

CAP traces are from baseline (black), aglycemia (red) and recovery (dotted black) conditions (**A**) and L-lactate application during aglycemia (**B**). Note that P1 representing myelinated axons and P2 representing unmyelinated axons are the two peaks observed in CC CAP recordings. CAP area is quantified by measuring the area above the blue dotted lines and the response. (**C** and **D**).

Application of L-lactate (dark red) during aglycemia in aging CC preserved axonal function when compared to glucose (pink). (**E**) Time course displays CAP area changes when aging MON (red) and aging CC (pink) were exposed to 1 h aglycemia. (**F**) CAP area recovery in CC is higher compared to MON. (**G**) During aglycemia, CC axons were more resilient than MON axons. CAP area from CC slices at the end of aglycemia (red arrow, D and F) was higher when compared to MONs. *** $p < 0.001$ **** $p < 0.0001$, unpaired Student's

two-tailed t-test. (For interpretation of the references to colour in this figure legend, the reader is referred to the web version of this article.)

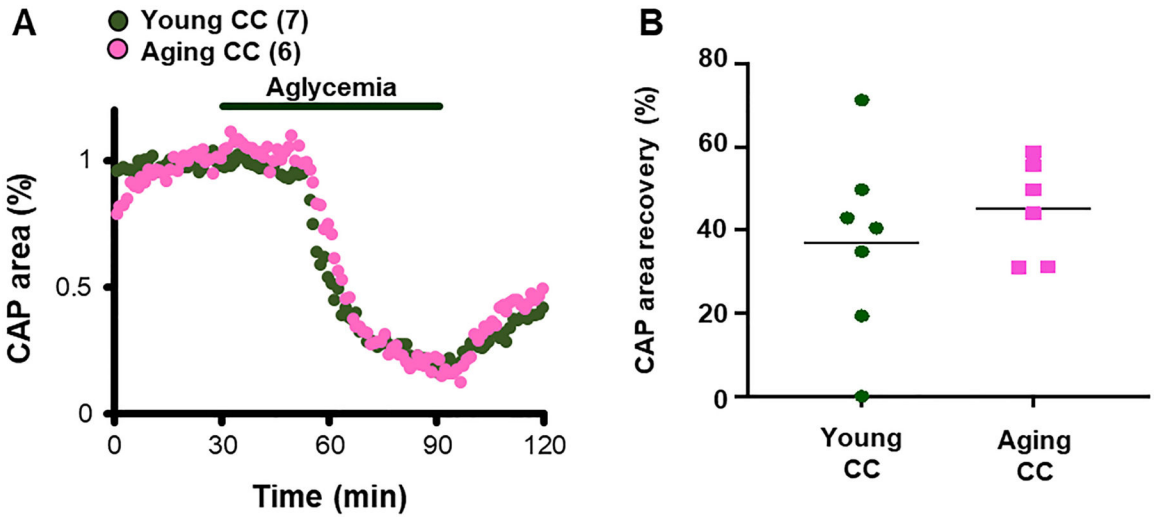

Fig. 8. Young and aging corpus callosum axons are equally resilient to aglycemia.

(**A**) Time course displays CAP area changes when Young CC (green) and Aging CC (pink) slices were exposed to 1 h aglycemia. **(B)** CAP Area recovery was comparable in both young and aging CC after aglycemia. ns $p > 0.05$, Unpaired Student's two-tailed t-test. (For interpretation of the references to colour in this figure legend, the reader is referred to the web version of this article.)